Chemical Papers (2020) 74:3755–3766
https://doi.org/10.1007/s11696-020-01257-4

ORIGINAL PAPER

The crystal structure of tetrameric copper(II) complexes, Hirshfeld surface analysis, and vector analyses of $Cu_4OCl_6L_4$ complexes with N-donor ligands

Gregor Ondrejovič[1] · Ján Moncol[1] · Marian Koman[1]

Received: 14 February 2020 / Accepted: 18 June 2020 / Published online: 23 June 2020

Abstract

It is known, that in the $Cu_4OX_6L_4$ (X = Cl, Br) complexes can be present many different ligands L, including bioligands. The synthesis and characterization of $Cu_4OBCl_6(ron)_4$ (**1**) and $Cu_4OCl_6(3\text{-Mepy})_4$ (**2**) (where ron is ronicol or 3-methanolpyridine and 3-Mepy is 3-methylpyridine) are reported. The complexes under study were X-ray structure analysis and Hirshfeld surface analysis. Tetranuclear $Cu_4OX_6L_4$ complexes with molecular structure (Fig. 1) can help to better understand the role of donor–acceptor and electron-transfer properties in copper proteins. The coordination sphere about each copper(II) atom is trigonal bipyramidal with three chlorine atoms in the equatorial plane. The apical positions are occupied by the central oxygen atom and the nitrogen atom of the respective ligand ($CuCl_3ON$). Here are studied chloridocomplexes of some *N*-donor ligands, L = *chloro-promazine, ronicol (3-pyridylmethanol)*, *2-ethylpyrazine*, seven *derivatives of pyrazol* and for comparisons *3-methylpyridine*. The $Cu_4OCl_6L_4$ molecule is regarded as a supramolecular model of interactions between bioligand L and hypothetical "round-shaped" coordination tetra-receptor Cu_4OCl_6. Vector calculations applied usualy to mechanical and electrical macroconstructions are here applied to microconstructions represented by structures of $Cu_4OX_6L_4$ molecules. For vector calculations each $Cu_4OX_6L_4$ structure is placed (Fig. 1) into the three-dimensional Cartesian coordinate system with the central oxygen atom O1 placed in its origin 0. Studied bioligands are compared and described by molecular structural dynamics and corresponding shifts of electron densities by means of bond lenghts (O1–Cu, Cu–L, Cu–X) and structural distances (O1···X, O1···L).

Keywords Crystal structure · Tetramers · Vector analyses · Copper(II) complexes · Hirshfeld surface

Introduction

Over 40 crystal structures tetranuclear copper(II) complexes of type $Cu_4OX_6L_4$, which various ligand L are known. Selected structural parameters for $Cu_4OCl_6(NL)_4$ complexes [NL = ligand with nitrogen donor atom, such as derivatives of amine (Becker et al. 2015; Bowmaker et al. 2011; Löw et al. 2013), pyridine (El-Toukhy et al. 1984; Gill and Sterns 1970; van Albada et al. 2011; Zhang et al. 2014), pyrazine (Näther and Jess 2002), pyrazole (Kashyap et al. 2013; Keij et al. 1991; Vafazadeh et al. 2015; Vafazadeh and Willis 2016), imidazole (Atria et al. 1999, Betanzos-Lara et al. 2012, Cortes et al. 2006, Jian et al. 2004, Lobana et al. 2011, Tosik et al. 2009), triazole (Richardson and Steel 2003; Skorda et al. 2005; Voitekhovich et al. 2009), and others (Kariuki and Newman 2018)], are summarized in the review by Melník and co-authors (Melník et al. 2011). The coordination sphere about each copper(II) atom is trigonal

This work was presented at the International Conference on Coordination and Bioinorganic Chemistry held in Smolenice on June 2–7, 2019.

Electronic supplementary material The online version of this article (https://doi.org/10.1007/s11696-020-01257-4) contains supplementary material, which is available to authorized users.

✉ Ján Moncol
jan.moncol@stuba.sk

[1] Faculty of Chemical and Food Technology, Institute of Inorganic Chemistry, Technology and Materials, Slovak University of Technology, Radlinského 9, 812 37 Bratislava, Slovakia

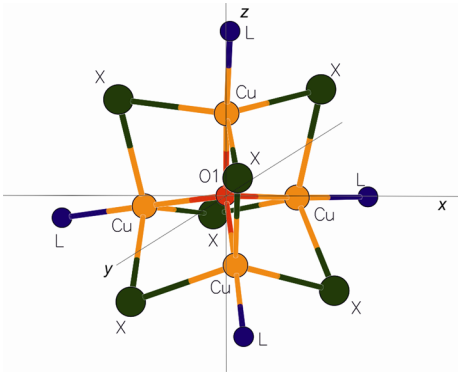

Fig. 1 Structure of the $Cu_4OX_6L_4$ molecule

bipyramidal with three chlorine atoms in the equatorial plane. The apical positions are occupied by the central oxygen atom and the nitrogen atom of the respective ligand ($CuCl_3ON$). The equatorial plane is much less crowded than the apical sides, with mean Cu–Cl_{eq} bond distances of 2.41 (range 2.325–2.46) Å and the mean Cu–O_{ap} and Cu–N_{ap} bond distances of 1.905 (range 1.89–1.92) Å and 1.97 (range 1.930–2.025) Å. The mean Cu•••Cu separation of 3.110 Å (range from 3.090 to 3.133 Å) excludes a direct metal–metal bond. The deviation of the mean tetrahedral Cu–μO–Cu bond angle is from the ideal value of 109.5° (range 0.3–6.4°). The Cu–μCl–Cu bond angle ranges from 76.7 to 82.7° (mean 80.4°).

The vector analysis never been applied to chemical objects represented by molecular structures before (Červeň 2015; Cikunov 1973). Figures 2 and 3 clearly demonstrate positions of bonds Cu–O, Cu–N and Cu–Cl in the structures. These bonds form polyhedra: tetrahedron OCu_4 and four trigonal bipyramids $OCuCl_3N$. The bonds O–Cu participate in both types of polyhedra. The central oxygen atom O of

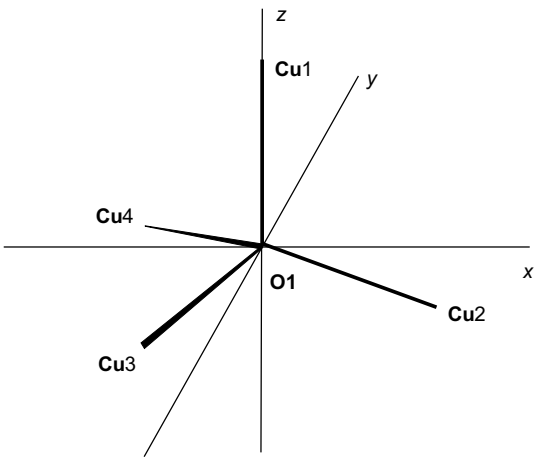

Fig. 2 The bond equivalent tetetrahedron O1–Cu_4 is represented by four bonding vectors

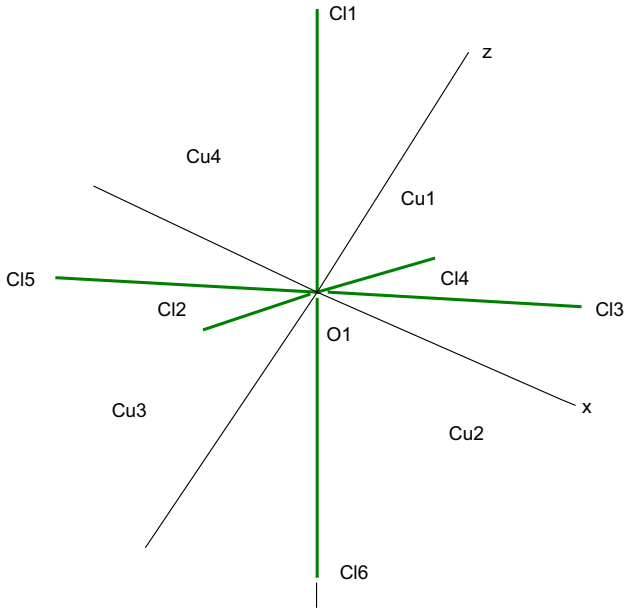

Fig. 3 The non-bonding distance equivalent octahedron O1•••X_6 is represented by six distance vectors $O1\bullet\bullet\bullet > X$ giving total octahedron vector O_X. For ideal octahedron, $O_X = 0$

O–Cu bonds has a unique structural position, since, besides mentioned polyhedra, it participates in six O•••Cl distances that form the OCl_6 octahedral system. Tetrahedron OCu_4 is bonding homogeneous (equivalent), its four bonds O–Cu are of the same kind. Similarly, the polyhedral systems OCl_6 are homogeneous (equivalent) by distances OCl_6. By sum of four bond vectors O–Cu, the tetrahedral vector T_{Cu} can be calculated, by sum of six distance vectors O…Cl the octahedral vector O_{Cl}.

The trigonal bipyramid $OCuCl_3N$ is bonding non-homogeneous unit. However, it is composed of the bonding homogeneous equatorial $CuCl_3$ subunit and the bonding non-homogeneous axial O–Cu–N subunit. Each of the bonds Cu–Cl and Cu–N must be transformed to bond vectors in the orthogonal coordinate system with x, y, and z axes. The transformed bond vectors serve for calculation of the equatorial E_{Cl} and axial A_{ON} vectors. From these subunit vectors, the total polyhedral trigonal bipyramidal vector P_{Cu} can be calculated. Most complex vector is represented by the total molecular $Cu_4OCl_6N_4$ vector. This vector can be obtained by summing of four trigonal bipyramidal $OCuCl_3N$ vectors, P_{Cu}.

For transformation of the bonds and interatomic distances to bond vectors and distance vectors, respectively, the molecular structure is placed into orthogonal coordinate system with atom O in the origin of coordinate axes x, y, z. One of the O–Cu bonds, mostly O–Cu1, is placed into $+z$ axis and other O–Cu bond, mostly O–Cu2, into x, $-z$ plane, as shown in Fig. 2. After transformation, each of the vectors

has its origin in the axes origin and the end point is defined by calculated coordinates *x*, *y*, *z*. The distance between the origin and the end point measured in *pm* is a vector magnitude, in this case, vector length. The direction of the vector is represented by the vector coordinates *x*, *y*, *z*.

Polyhedron vectors of tetrahedron T_{Cu} and octahedron O_{Cl} are calculated from vectors of transformed bonds and distances according to the equations:

$T_{Cu} = \Sigma(O1 - Cu(1-4))$.

$O_{Cl} = \Sigma(O1 \ldots Cl(1-6))$.

For trigonal bipyramid $O_1Cu_1Cl_3N_1$:

$P_{Cu1} = E_{Cl} + A_{O1N1}$.

E_{Cl} = equatorial vector of bonds Cu_1Cl_3.

A_{O1N1} = axial vector of bonds O1–Cu1 and Cu1–N1(L).

The principles of vector methods and calculations are described in literature (Ondrejovič and Moncol 2015, 2017).

The use of the orthogonal coordinate system with the origin occupied by atom O of the OCu_4 tetrahedron corresponds to the Schoenflies molecular structure parameter T_d and electron bonds representations of the OCu_4 tetrahedral-bonding system. Both aspects, crystallographic and chemical, are connected by the same point group.

The $Cu_4O_1X_6L_4$ structure consists of two basic polyhedra: $O1 \rightarrow Cu$ giving total tetrahedron vector T_{Cu}. For ideal tetrahedron, $T_{Cu} = 0$.

Four trigonal bipyramidal coordination polyhedra (Fig. 4) of central copper(II) atoms are strongly bonding nonequivalent. Therefore, $TB_{Cu} > 0$.

The vector analyses have also been applied to ten structures of the $Cu_4OCl_6L_4$ complex molecules with L = *N*-donor ligands. Presented results demonstrate correlations between structural molecular parameters and supramolecular inner- and intermolecular contacts by hydrogen bonds and van der Waals interactions.

Structures of $Cu_4OX_6L_4$ complexes are of considerable interest, since about 116 structures are registered in the CCDC database (Groom et al. 2016).

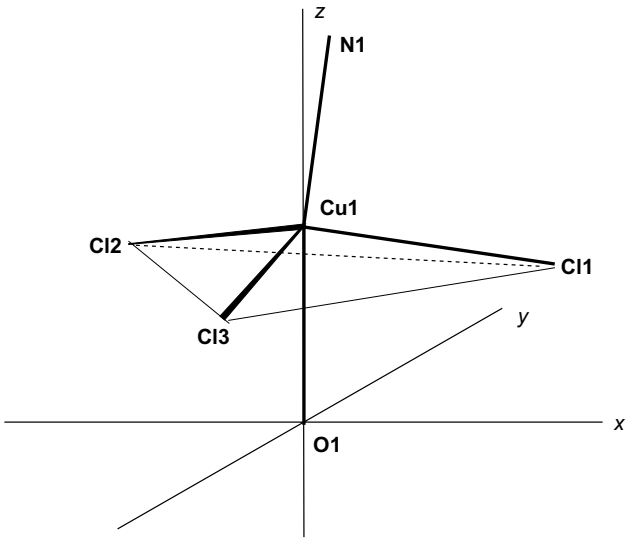

Fig. 4 The trigonal bipyramidal coordination polyhedra of central copper(II) atoms

Experimental

Synthesis of the complexes

Chemicals, syntheses and characterization of the $Cu_4OCl_6(ron)_4$ (1) complexes instruments have been described in our previous report (Koman and Ondrejovič 2013; Ondrejovič et al. 2006). Single crystals of the $Cu_4OCl_6(3\text{-Mepy})_4$ (**2**) complex were prepared by diffusion of the 3-Mepy ligand into a methanol solution of the $Cu_4OCl_6(methanol)_4$ complex as described elsewhere (Norman and Rose 1989; Löw et al. 2013) similar to the 1-methanolpyridine synthesis.

X-ray crystallography

Intensity data for $Cu_4OCl_6(ron)_4$ (**1**) were collected using a Siemens P4 diffractometer with graphite monochromated MoKα radiation (Siemens 1990). The diffraction intensities were corrected for Lorentz, polarization effects and absorption correction with XSCANS (Siemens XSCANS and XEMP 1994). Intensity data for $Cu_4OCl_6(3\text{-Mepy})_4$ (**2**) were collected using diffractometer Stoe StadiVari using Pilatus3R 300 K HPAD detector and microfocused X-ray source Xenocs Genix3D Cu HF (Cu K_α radiation) at 100 K. The structures were solved using the programs SIR–2011 (Burla et al. 2012) or SHELXT (Sheldrick 2015a) and refined by the full-matrix least-squares method on all F^2 data using the program SHELXL–2018/3 (Sheldrick 2015b). Geometrical analysis was performed using SHELXL–2018/3. The structures were drawn by OLEX2 (Dolomanov et al. 2009) software.

Crystal data and conditions of da collection and refinement for complexes **1** ad **2** are reported in Table 1.

Hirshfeld surface analysis

Hirshfeld surface analysis (Hirshfeld 1977; Spackman and Jayalitaka 2009) and associated fingerprint plots (Parkin et al. 2007; Spackman et al. 2002) have been made using program CrystalExplorer (version 17.5) (Turner et al. 2017). The Hirshfeld surface of **1** has been calculated including all orientations of the disordered molecule with their partial occupancies.

Table 1 Crystal data and structure refinement for complexes **1** and **2**

	$Cu_4OCl_6(ron)_4$—**1**	$Cu_4OCl_6(3\text{-Mepy})_4$—**2**
Chemical formula	$C_{24}H_{28}Cl_6Cu_4N_4O_5$	$C_{24}H_{28}Cl_6Cu_4N_4O$
M_r	919.41	855.36
Crystal system, space group	monoclinic, $P2_1/n$	orthorhombic, *P*bca
Temperature (K)	293(1)	100(1)
a	11.346(1) Å	12.8364(4) Å
b	15.807(2) Å	30.3137(8) Å
c	19.027(2) Å	16.3451(4) Å
α (°)	90	90
β (°)	106.27(3)	90
γ (°)	90	90
V (Å^3)	3275.8(6)	6360.2(3)
Z	4	8
Radiation type	0.71073 Å (Mo K_α)	1.54186 (Cu K_α)
2Θ range for data collection	8.36°–52.73°	5.832°–143.198°
Index ranges	$-1 \le h \le 14$, $-1 \le k \le 19$ $-23 \le l \le 23$	$-11 \le h \le 15$, $-37 \le k \le 27$, $-19 \le l \le 18$
μ (mm^{-1})	3.092	7.860
Crystal size (mm)	0.45 × 0.38 × 0.35	0.14 × 0.07 × 0.03
Diffractometer	Siemens P4	Stoe StadiVari
Absorption correction	Psi-scan	Multi-scan
Reflections collected	8250	52,601
Data/redtrains/parameters	6667/24/396	6003/0/356
R_{int}	0.0408	0.0783
$R[F^2 > 2\sigma(F^2)]$, $wR(F^2)$, S	$R_1 = 0.0657$ $wR_2 = 0.1953$	$R_1 = 0.0378$ $wR_2 = 0.0866$
S	1.011	0.907
Largest diff. peak and hole (e. Å^{-3})	1.05 and − 1.52	0.75 and − 0.41

Results and discussion

Crystal structures

Complex **1** crystallizes in monoclinic space group $P2_1/n$, and other hand compound **2** crystallizes in orthorhombic space group *P*bca. All copper atoms are joined by three μ_2-chlorido bridging ligands and one μ_4-oxido ligand. The coordination polyhedron around all copper atoms in both tetranuclear complexes is trigonal-bipyramide. The trigonal plane is built up by three chlorido ligands, and axial positions are occupied by one oxygen atom and one pyridine nitrogen atom of ronicol (3-hydroxymethylpyridine) (**1**) or 3-methylpyridine (**2**). The structures of title complexes $Cu_4OCl_6(ron)_4$—**1** and $Cu_4OCl_6(3\text{-Mepy})_4$—**2** can be described as a system of three penetrating polyhedral. These polyhedral, the OCu_4 tetrahedron, the OCl_6 octahedron, and four $CuOCl_3N$ trigonal bipyramids can be distorted due to both intramolecular and intermolecular interactions (Ondrejovič et al. 2000). Selected interatomic distances are listed in Table 2. The molecular structures of $Cu_4OCl_6(ron)_4$—**1** and $Cu_4OCl_6(3\text{-Mepy})_4$—**2** are shown in Fig. 5.

The crystal structures of **1** is drawn in Fig. 6. The molecules of $Cu_4OCl_6(ron)_4$ are connected through O–H•••O hydrogen bonds between hydroxyl oxygen atoms of 3-pyridylmethanol ligands [O2–H2•••O1, O2–H2•••O1A, O3–H3•••O4, O3–H3•••O4A, O4–H4•••O4 and O4A–H4A•••O4A, the O···O distances are in the range 2.74–3.06 Å (See ESI Table S1)] and O1–H1•••Cl5 hydrogen bond between hydroxyl oxygen atom of 3-pyridylmethanol ligand (O1) and chlorine atom (Cl5) [the distance of O1•••Cl5 [3.218(19)] Å, (See ESI Table S1)] and forming 3D supramolecular network (Fig. 6). The O–H•••O and O–H•••Cl hydrogen-bond system of **1** is enriched by weaker C23–H23•••O3 hydrogen-bonding interactions between carbon atom of pyridine ring (C23) and hydroxyl oxygen atom of 3-pyridylmethanol ligand (O3) [the distance of C23•••O3 (3.403(12)) Å, (See ESI Table S1)]; and C–H•••Cl hydrogen-bonding interactions between carbon atoms of pyridine ring (C33) or methylene group (C16, C46) of 3-pyridylmethanol ligands and chlorine atoms (Cl1, Cl4Cl3) [C16–H16B•••Cl1, C33–H33•••Cl4 and C46–H46B•••Cl3, the C···Cl distances are in the range 3.40–3.63 Å (See ESI Table S1)].

Table 2 Selected bond distances [Å] for complexes **1** and **2**

$Cu_4OBCl_6(ron)_4$—**1**			
Cu1–O1	1.916(4)	Cu1–N1	1.979(5)
Cu2–O1	1.909(4)	Cu2–N2	1.969(5)
Cu3–O1	1.909(4)	Cu3–N3	1.996(6)
Cu4–O1	1.916(4)	Cu4–N4	1.989(5)
Cu1–Cl3	2.363(2)	Cu3–Cl1	2.401(2)
Cu1–Cl4	2.402(2)	Cu3–Cl2	2.395(2)
Cu1–Cl6	2.452(2)	Cu3–Cl3	2.402(2)
Cu2–Cl2	2.386(2)	Cu4–Cl1	2.444(2)
Cu2–Cl4	2.447(2)	Cu4–Cl5	2.428(2)
Cu2–Cl5	2.471(2)	Cu4–Cl6	2.395(2)
$Cu_4OCl_6(3\text{-Mepy})_4$—**2**			
Cu1–O1	1.898(2)	Cu1–N1	1.979(3)
Cu2–O1	1.901(3)	Cu2–N2	1.983(3)
Cu3–O1	1.921(3)	Cu3–N3	1.980(3)
Cu4–O1	1.904(3)	Cu4–N4	1.969(3)
Cu1–Cl1	2.381(1)	Cu3–Cl2	2.400(1)
Cu1–Cl2	2.436(1)	Cu3–Cl4	2.395(1)
Cu1–Cl3	2.378(1)	Cu3–Cl6	2.361(1)
Cu2–Cl1	2.416(1)	Cu4–Cl3	2.398(1)
Cu2–Cl4	2.464(1)	Cu4–Cl5	2.391(1)
Cu2–Cl5	2.376(1)	Cu4–Cl6	2.486(1)

On the other hand, complex **2** forms also 3D supramolecular network (Fig. 7), but complex molecules $Cu_4OCl_6(3\text{-Mepy})_4$ are joined only via weak C–H•••Cl hydrogen-bonding interactions. The C–H•••Cl hydrogen-bonding interactions in crystal structure of **2** are observed between carbon atoms of pyridine ring (C3, C4) or methyl group (C12, C18, C24) of 3-methylpyridine ligands, and chlorine atoms (Cl3, Cl4C6) [C3–H3•••Cl6, C4–H4•••Cl3, C12–H12C•••Cl4, C18–H18C•••Cl4 and C24–H24B•••Cl6, the C···Cl distances are in the range 3.52–3.82 Å (See ESI Table S1)]. The crystal structure of **2** exhibits also π–π stacking interactions (Janiak 2000) between pyridine rings [N2/C7–C11)] and [N4/C19–C23] with centroid–centroid distance of 3.63 Å and shift distance of 0.63 Å.

Hirshfeld surface analysis

Hirshfeld surface analysis was used to further study the intermolecular interactions of the crystal structures of both compounds. Figures 8, 9 show the 3D Hirshfeld surface of **1** and **2**, respectively. The 3D Hirshfeld surfaces have been mapped over d_{norm} shape index (Figs. 8, 9). The surfaces are shown as transparent to allow visualization of the molecular moiety around which they were calculated. As shown in Figs. 8, 9, the deep red spots on the d_{norm} Hirshfeld surfaces indicate the close-contact interactions, which are mainly

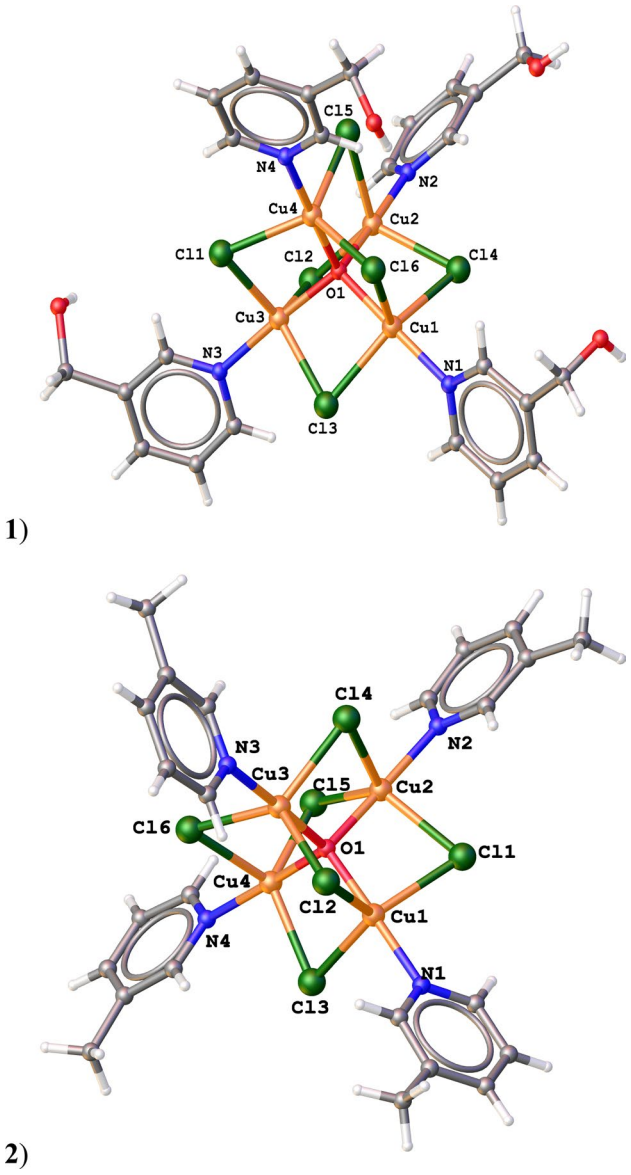

Fig. 5 Molecular structures of the $Cu_4OCl_6(ron)_4$—**1** and $Cu_4OCl_6(3\text{-Mepy})_4$—**2**

responsible for the significant intermolecular hydrogen-bonding interactions.

The 3D Hirshfeld surface illustration of **1** (Fig. 8) shows the deep red areas representing O–H•••O, O–H•••Cl, and also weaker C–H•••Cl hydrogen-bonding interactions. The 3D Hirshfeld surface illustration of **2** (Fig. 9) also shows weaker C–H•••Cl hydrogen-bonding interactions. The Hirshfeld surface plotted over shape index of **2** visualizes the π–π stacking interactions (Janiak 2000) by the presence of adjacent red and blue triangles (Fig. 9).

The Hirshfeld 2D fingerprints of **1** and **2** compounds are illustrated in supplementary material (See ESI Figs. S3 and S4). The Hirshfeld 2D fingerprint plots allow a

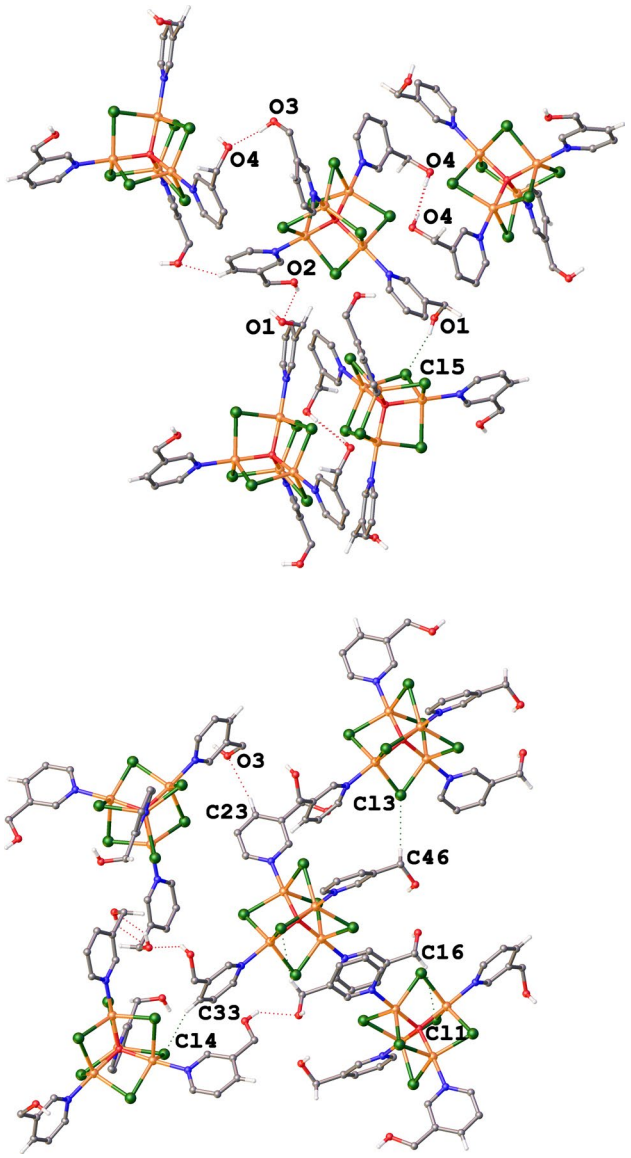

Fig. 6 The hydrogen-bonding network in crystal structure of $Cu_4OCl_6(ron)_4$ (**1**). The stronger O–H•••O and O–H•••Cl hydrogen bonds are drawn in top. The weaker C–H•••O and C–H•••Cl hydrogen-bonding interactions are pictured in bottom

quick and easy identification of the significant intermolecular interaction map on the molecular surface. As shown in Fig. S3 in supplementary materials, the strong H•••O/O•••H, and weak H•••C/C•••H, and H•••Cl/Cl•••H hydrogen-bonding interactions cover the 10.0, 10.1 and 22.8%, respectively, of the total Hirshfeld surface with two distinct spikes in the 2D fingerprint plots, indicating hydrogen-bonding interactions are the most significant interactions in the crystal. As shown in Fig. S3 in supplementary material, in the middle of scattered points in the 2D fingerplots, H•••H interactions cover 42.0% of the total Hirshfeld surface. As shown in Fig. S4 in supplementary

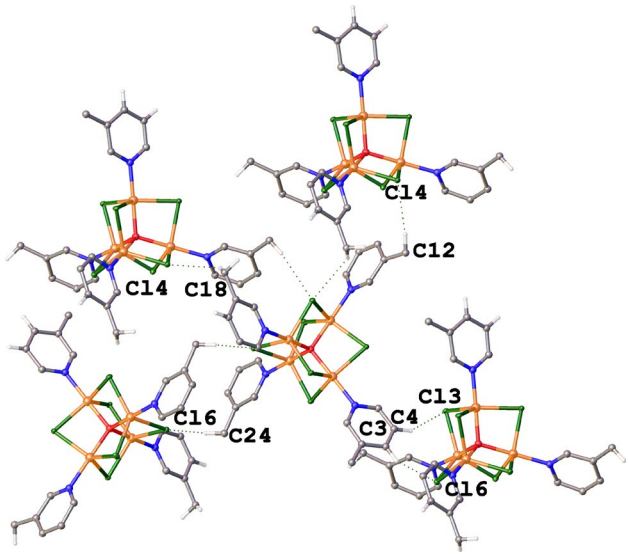

Fig. 7 The weak C–H•••Cl hydrogen-bonding interactions in crystal structure of $Cu_4OCl_6(3\text{-Mepy})_4$ (**2**)

material, in scattered points in the 2D fingerplots, H•••C/C•••H and H•••Cl/Cl•••H interactions cover in the 17.5 and 29.1%, respectively, of the total Hirshfeld surface. In scattered points of the 2D fingerplot in **2** (See Fig. S4), H•••H and C•••C interactions illustrate covering of 43.3 and 2.5%, respectively.

Vector analysis

Analyzed ten structures of the $Cu_4OCl_6L_4$ complexes are presented in Table 3. The structures are characterized by crystallographic data including codes of CCDC database. Calculated vector parameters of tetrahedron *TCu*, octahedron *OCl*, trigonal bipyramids Cu1, Cu2, Cu3, Cu4, and corresponding molecule MOL are characterized by length and sector of the three-dimensional Cartesian coordinate system (three combined symbols of + and −). Intramolecular and intermolecular interactions are demostrated by similar way. Red symbols demonstrate the identical directions.

The results presented in Tables 3, 4 are not surprising because of strong differences in bioactivity of ligands L. There is some clasification of bioactive ligands L through the graphical comparison of vectors in Dependence 1 (See ESI Fig. S3) and Dependence 2 (See ESI Fig. S4). In Dependence 1, it is clearly seen how correspond tetrahedral T_{Cu}, octahedral O_{Cl}, and molecular *MOL* vectors. It is clearly seen that disorders have very weak influence on vector data. However, in Dependence 2, it is clearly seen that molecular interactions for complexes 4A, 4B are different, for complexes 5A, 5B very diferent, but for complexes 6A, 6B, there is practicaly no diference.

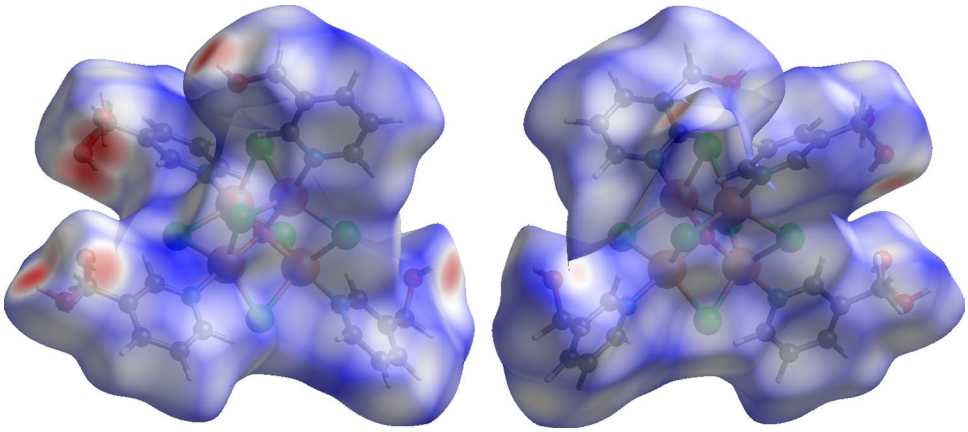

Fig. 8 View of the three-dimensional Hirshfeld surface of **1** plotted over d_{norm} in the range − 1.1524 to 1.2567 a.u

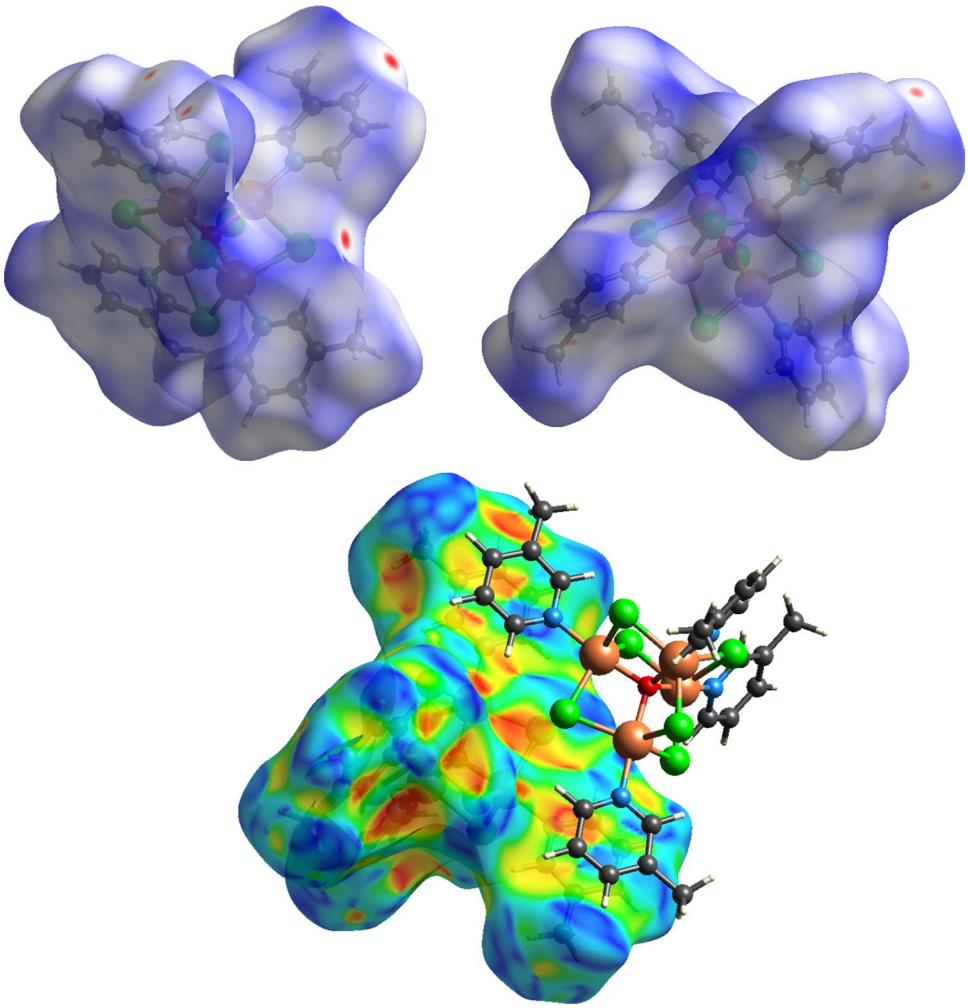

Fig. 9 View of the three-dimensional Hirshfeld surface of **2** plotted over d_{norm} in the range − 0.0827 to 1.6290 a.u. (top) and shape index (bottom)

Conclusions

1. The crystal structure of both complexes shows 3D supramolecular networks. The 3D supramolecular network of $Cu_4OCl_6(ron)_4$ (**1**) is formed through O–H•••O, O–H•••Cl, and C–H•••Cl hydrogen bonds. The C–H•••Cl hydrogen bonds form the 3D supramolecular network of $Cu_4OCl_6(3\text{-Mepy})_4$ (**2**). The chlorine atoms of both complexes are acceptors of hydrogen bonds, which are also confirmed by Hirshfeld surfaces analysis.

Table 3 Ligands and crystallographic data of selected $Cu_4OCl_6L_4$ complexes, where L = *N*-donor ligands

LIGAND L NUMBER	LIGAND L SOLVATE, Disorder	CRYSTALLOGRAPHIC DATA, Refcode
1	*Chlor-promazine* $4.C_6H_6$	Monoclinic $P2_1/a$ $R = 6.5\%$ PIVHAD (Yamada et al. 1994)
2A	*3-Pyridylmethanol, ronicol* A: O1-H1, O4-H4 Disorder	Monoclinic $P2_1/n$ $R = 6.57\%$ (This paper—**1**)
3	*2-Ethylpyrazine*	Monoclinic $P2_1/n$ R = 3.56% IDICUT (Nather et al. 2002)
4A	*3,5-Dimethylpyrazole* A: Cl4 Disorder	Monoclinic *P2/n* R = 3.9% BOGCEG (Stibrany et al. 2007)
4B	*3,5-Dimethylpyrazole* B: Cl4A Disorder	Monoclinic *P2/n* $R = 3.9\%$ BOGCEG (Stibrany et al. 2007)
5A	*3,5-Dimethylpyrazole* $4.C_2H_5OH$ A: Cl6, *Oc: 0.6* Disorder	Triclinic *P-1* $R = 8.3\%$ RIRKOT (Jacimovic et al. 2007)
5B	*3,5-Dimethylpyrazole* $4.C_2H_5OH$ B: Cl7, *Oc: 0.4* Disorder	Triclinic *P-1* $R = 8.3\%$ RIRKOT (Jacimovic et al. 2007)
6A	*3,5-Diisopropyl-1H- pyrazole* A: Cl4, *Oc: 0.5* Disorder	Monoclinic *C2/c* $R = 3.03\%$ $T = 100$ K DIFTIX (Kashyap et al. 2013)
6B	*3,5-Diisopropyl-1H- pyrazole* B: Cl4A, *Oc: 0.5* Disorder	Monoclinic *C2/c* $R = 3.03\%$ $T = 100$ K DIFTIX (Kashyap et al. 2013)
7	*3,4-Dimethyl-5-phenyl-pyrazole*	Monoclinic *I2/a* $R = 5.2\%$ JIWKAB (Keij et al. 1991)
8	*5-(2,4,6-Trimethyl-phenyl)pyrazole*	Monoclinic *C2/c* $R = 3.6\%$ WUXBOG (Liu et al. 2003)
9	*3-Methyl-5-phenyl-1H-pyrazole*	Tetragonal *P4/n* $R = 6.65\%$ IJIWII (He 2011)
10	*3-Methylpyridine*	Orthorhombic *Pbca* $R = 3.78$ (This paper—**2**)

Table 4 Vector and interaction parameters [*pm*] for structure of selected $Cu_4OCl_6L_4$ complexes L = *N*-donor ligands

Ligand	Tetra	Octa	Trigonal polyhedron				Molecule
L	T_{Cu}	O_{Cl}	Cu1	Cu2	Cu3	Cu4	MOL
1	11.14	16.70	62.35	59.69	61.12	59.37	26.45
	(− − −)	(− − −)	(− − −)	(−++)	(+ − +)	(+++)	(−++)
	Interactions		1112.1	2301.1	1835.5	1431.1	3006.4
			(−++)	(+++)	(−+−)	(−+−)	(−+−)
2A	4.81	47.23	329.08	322.10	322.23	329.30	98.65
	(+ − −)	(−++)	(−++)	(++−)	(− − −)	(−+−)	(+++)
	Interactions		1319.85	563.69	637.72	870.25	1364.79
			(+++)	(− − −)	(− − +)	(− +−)	(−++)
3	2.10	30.09	329.40	324.40	323.16	320.55	67.13
	(+ − +)	(− − +)	(−++)	(++−)	(− − −)	(−+−)	(−++)
	Interactions		990.64	825.74	883.63	829.35	772.31
			(−++)	(+ − −)	(− − −)	(−+−)	(−+−)
			Cu1	*Cu2*	*Cu1A*	*Cu2A*	
4A	4.55	79.41	325.81	322.30	321.33	322.32	157.34
	(− − +)	(−+−)	(−++)	(++−)	(− − −)	(−+−)	(−+−)
	Interactions		826.79	690.82	765.48	529.20	471.02
			(+++)	(++−)	(− − −)	(−++)	(++−)
4B	4.66	79.39	321.33	322.30	325.22	322.32	157.34
	(− − +)	(+ − −)	(+ − +)	(++−)	(− − −)	(−+−)	(+ − −)
	Interactions		957.93	695.40	659.23	528.16	904.66
			(+++)	(+ − −)	(− − −)	(− ++)	(+++)
5A	13.78	96.53	321.33	324.68	321.19	321.22	185.65
	(−+−)	(++−)	(+ − +)	(++−)	(−+−)	(− − −)	(++−)
	Interactions		662.62	265.67	648.86	734.25	445.33
			(+++)	(+ − +)	(− +−)	(− − −)	(+++)
5B	13.78	101.95	321.33	324.68	323.09	323.71	213.48
	(− +−)	(−++)	(+ − +)	(++−)	(− +−)	(− − −)	(− − +)
	Interactions		850.61	461.40	907.42	656.08	1636.93
			(−++)	(+ − +)	(− ++)	(− − +)	(−++)
			Cu1	*Cu2*	*Cu1A*	*Cu2A*	
6A	9.56	69.18	326.14	325.60	314.18	325.59	142.94
	(−++)	(− − −)	(− − +)	(+− −)	(− +−)	(− − −)	(− − −)
	Interactions		231.87	788.21	298.31	898.07	519.66
			(−+−)	(++−)	(+++)	(− − −)	(+− −)
6B	9.56	69.18	314.42	325.60	325.92	325.59	142.88
	(−++)	(− − −)	(+++)	(+− −)	(−+−)	(− − −)	(+ − −)
	Interactions		298.41	788.21	231.28	898.07	500.48
			(−+−)	(++−)	(− ++)	(− − −)	(− − −)
			Cu1	*Cu2*	*Cu1B*	*Cu2B*	
7	2.24	6.24	322.76	327.00	322.78	327.03	14.62
	(+ − −)	(+ − −)	(− − +)	(++−)	(− +−)	(− − −)	(+− −)
	Interactions		749.94	1473.63	677.10	1473.16	494.07
			(+ − +)	(+ − +)	(+ − −)	(−+−)	(+ − +)
8	6.95	8.90	327.80	318.88	327.78	318.87	45.59
	(++−)	(− − +)	(− − +)	(++−)	(− − −)	(− +−)	(− − +)
	Interactions		1137.55	878.87	1179.03	878.76	974.48
			(− − +)	(+ − −)	(+ − +)	(−++)	(− − +)
			Cu1	*Cu1A*	*Cu1F*	*Cu1G*	
9	0.02	0.05	325.86	325.85	325.90	325.85	0.06
	(+0+)	(− − +)	(+++)	(+ − −)	(− − −)	(− + −)	(− − −)

Table 4 (continued)

Ligand	Tetra	Octa	Trigonal polyhedron				Molecule
	Interactions		698.18	698.29	698.28	698.30	0.28
			(− − +)	(+ + −)	(− − −)	(− + −)	(+ + −)
10	3.92	74.68	327.03	320.30	337.94	320.41	170.85
	(− − −)	(− + −)	(− + +)	(+ + −)	(− + −)	(− − −)	(− + −)
	Interactions		565.48	741.59	502.04	741.33	1220.29
			(− − +)	(+ + −)	(− + −)	(− + −)	(− + −)

2. The Hirshfeld surfaces analysis of $Cu_4OCl_6(3\text{-Mepy})_4$ (**2**) confirms also π–π stacking interactions between pyridine rings.
3. This paper presents structural data of two tetrameric copper(II) complexes which contain a μ_4-oxo group tetrahedrally coordinated to four copper(II) centers. Each pair of copper(II) centers is bridged by a single chlorine atoms. The coordination sphere about each copper(II) is trigonal–bipyramidal, which three chlorine atoms in the trigonal plane. One apical position about each copper(II) is occupied by oxygen atom, which is tetrahedrally coordinated to four copper(II) atoms. The second axial position is occupied by ligands with nitrogen donor atom.
4. The vector analyses combine chemical and structural aspects of coordination compounds into one quantitative parameter—structural vector which is correlated with intra- and intermolecular interactions. As a method of crystallochemistry, it can be applied to arbitrary molecule.
5. Structural vector parameters of biomolecules L coordinated to Cu_4OX_6 receptors provide usefull quantitative informations about possible interaction activity of biomolecules in the real bioenvironment.
6. Vectors of nonvalence supramolecular, hydrogen bond, and Van der Waals interactions correlate with the bond vectors of tetrahedrons OCu_4, distance vectors of octahedrons OCl_6, and total molecular vectors in molecular structures of $Cu_4OX_6L_4$ complexes.

Acknowledgements The authors would like to thank Grant agencies of the Slovak Republic (VEGA 1/0639/18, APVV-18-0016) are gratefully acknowledged for their financial support. This article was created with the support of the MŠVVaŠ of the Slovak Republic within the Research and Development Operation Program for the project "University Science Park of STU Bratislava" (ITMS project no. 26240220084) cofounded by the European Regional Development Fund.

References

Atria AM, Vega A, Contreras M, Valenzuela J, Spodine EC (1999) Magnetostructural characterization of μ_4-oxahexa-μ_2-chlorotetrakis(imidazole)copper(II). Inorg Chem 38:5681–5685. https://doi.org/10.1021/ic990389

Becker S, Behrens U, Schindler S (2015) Investigations concerning $[Cu_4OX_6L_4]$ cluster formation of copper(II) chloride with amine ligands related to benzylamine. Eur J Inorg Chem 2015:2437–2447. https://doi.org/10.1002/ejic.201500115

Betanzos-Lara S, Gomez-Ruiz C, Barron-Sosa LR, Gracia-Mora I, Flores-Alamo M, Barba-Behrens N (2012) Cytotoxic copper(II), cobalt(II), zinc(II), and nickel(II) coordination compounds of clotrimazole. J Inorg Biochem 114:82–93. https://doi.org/10.1016/j.jinorgbio.2012.05.001

Bowmaker GA, Nicola CD, Marchetti F, Pettinari C, Skelton BW, Somers N, White AH (2011) Synthesis, spectroscopic and structural characterization of some novel adducts of copper(II) salts with unidentate nitrogen bases. Inorg Chim Acta 375:31–40. https://doi.org/10.1016/j.ica.2011.04.005

Burla MC, Caliandro R, Camalli M, Carrozzini B, Cascarano GL, Giacovazzo C, Mallamo M, Mazzone A, Polidori G, Spagna R (2012) SIR2011: a new package for crystal structure determination and refinement. J Appl Crystallogr 45:357–361. https://doi.org/10.1107/S0021889812001124

Červeň I (2015) Fyzika po kapitolách 1 Vektory. Vydavateľstvo Fakulty elektrotechniky a informatiky STU, Bratislava

Cikunov E (1973) Zbierka matematických vzorcov. ALFA, vydavateľstvo technickej a ekonomickej literatúry, Bratislava

Cortes P, Atria AM, Garland MT, Baggio R (2006) Three oxo complexes with a tetranuclear $[Cu_4(\mu_2\text{-}Cl)_6(\mu_4\text{-}O)]$ unit. Acta Crystallogr Sect C 62:m311–m314. https://doi.org/10.1107/S0108270106021354

Dolomanov OV, Bourhis LJ, Gildea RJ, Howard JAK, Puschmann H (2009) *OLEX2*: a complete structure solution, refinement and analysis program. J Appl Crystallogr 42:339–341. https://doi.org/10.1107/S0021889808042726

El-Toukhy A, Cai GZ, Davies G, Gilbert TR, Onan KD, Veidis D (1984) Transmetalation reactions of tetranuclear copper(II) complexes. 2. Steichiometry and products of reactions of $[(DENC)CuCl]_4O_2$, $[(DENC)CuCl]_4(CO_3)_2$, $[(DENC)CuCl]_4Cl_4$, and $(DENC)_4Cu_4Cl_6O$ complexes (DENC = *N*, N-diethylnicotinamide) with Ni(NS)2 complexes (nS is an S-methyl hydrazinecarbodithioate Schiff Base), the kinetics of product isomerization in aprotic solvents, and inhibition of copper-catalyzed phenolic oxidative coupling by dioxygen through transmetalation. J Am Chem Soc 106:4596–4605. https://doi.org/10.1021/ja00328a050

Gill N, Sterns M (1970) The preparation and properties of μ_4-oxohexa-μ-chloro-tetrakis[(2-methylpyridine)copper(II)] hydrate, $Cu_4OCl_6(2\text{-mepy})_4{\cdot}xH_2O$, and di-μ-methoxo-bis[chloro)2-methylpyridine)copper(II)], $[CuCl(OCH_3)(2\text{-mepy})]_2$, and X-ray structure analysis of $Cu_4OCl_6(2\text{-mepy})_4{\cdot}xH_2O$. Inorg Chem 9:1619–1625. https://doi.org/10.1021/ic50089a004

Groom CR, Bruno IJ, Lightfoot MP, Ward SC (2016) The cambridge structural database. Acta Crystallogr Sect B 72:171–179. https://doi.org/10.1107/S2052520616003954

He HS (2011) Hexa-μ_2-chlorido-μ_4-oxido-tetrakis[(3-methyl-5-phenyl-1*H*-pyrazole-κN^2)copper(II)]. Acta Crystallogr Sect E E 67:m 140. https://doi.org/10.1107/S1600536810053663

Hirshfeld FL (1977) Bonded-atom fragments for describing molecular charge densities. Theor Chim Acta 44:129–138. https://doi.org/10.1007/BF00549096

Jacimovic ZK, Leovac VM, Tomic ZD (2007) Crystal structure of hexakis(μ_2-chloro)-μ_4-oxo-tetrakis((3,5-dimethyl-pyrazole) copper(II)) ethanol tetrasolvate, $Cu_4OCl_6(C_5H_8N_2)_4 \bullet 4C_2H_5OH$. Z Kristallogr New Cryst Struct 224:246–248. https://doi.org/10.1524/ncrs.2007.0103

Janiak C (2000) A critical account on π-π stacking in metal complexes with aromatic nitrogen-containing ligand. J Chem Soc Dalton Trans 2000:3885–3896. https://doi.org/10.1039/B003010 0

Jian FF, Zhao PS, Wang HX, Lu LD (2004) Hydrothermal synthesis, crystal structure and EPR property of tetranuclear copper(II) cluster $[Cu_4OCl_6(C_{14}H_{12}N_2)_4]$. Bull Korean Chem Soc 25:673–675. https://doi.org/10.5012/bkcs.2004.25.5.673

Kariuki BM, Newman PD (2018) Asymmetric cationic phosphines: synthesis, coordination chemistry, and reactivity. Inorg Chem 57:9554–9563. https://doi.org/10.1021/acs.inorgchem.8b01657

Kashyap S, Singh UP, Singh AK, Kumar P, Singh SP (2013) Synthesis and structural studies of some copper-benzoate complexes. Transit Met Chem 38:573–585. https://doi.org/10.1007/s11243-013-9725-5

Keij FS, Haasnoot JG, Oosterling AJ, Reedijk J, Connor CJO, Zhang JH, Spek AL (1991) A pyrazole ligand yielding both chloro-bridged dinuclear and tetranuclear copper(II) compounds. The crystal and molecular structure of bis[μ-chloro-chloro(3,4-dimethyl-5-phenylpyrazole) (4,5-dimethyl-3-phenylpyrazole) copper(II)] and of (μ_4-oxo)hexakis(μ-chloro)tetrakis(3,4-dimethyl-5-phenylpyrazole)tetracopper(II). Inorg Chim Acta 181:185–193. https://doi.org/10.1016/S0020-1693(00)86809-7

Koman M, Ondrejovič G (2013) Ligand ronicol, which brings together and divides. Adv Sci Eng Med 5:598–602. https://doi.org/10.1166/asem.2013.1327

Liu XM, Kilner CA, Halcrow MA (2003) Hexa-μ_2-chloro-μ_4-oxo-tetrakis{[5-(2,4,6-trimethylphenyl)pyrazole-κN^2]copper(II)}. Acta Crystallogr Sect C 59:m100–m102. https://doi.org/10.1107/S0108270103002853

Lobana TS, Sultana R, Butcher RJ (2011) A sandmeyer type reaction for bromination of mercapto-1-methyl-imidazoline ($N_2C_4H_6S$) into 2-bromo-1-methyl-imidazole ($N_2C_4H_5Br$) in presence of copper(II) bromide. Dalton Trans 40:11382–11384. https://doi.org/10.1039/C1DT11327E

Löw S, Becker J, Würtele C, Miska A, Kleeberg C, Behrens U, Walter O, Schindler S (2013) Reactions of copper(II) chloride in solution: facile formation of tetranuclear copper clusters and other complexes that are relevant in catalytic redox processes. Chem Eur J 19:5342–5351. https://doi.org/10.1002/chem.201203848

Melník M, Koman M, Ondrejovič G (2011) Tetramers $Cu_4(\mu_4\text{-}O)(\mu\text{-}X)_6(L_4)$: analysis of structural data. Coord Chem Rev 255:1581–1586. https://doi.org/10.1016/j.ccr2010.12.005

Nather C, Jess I (2002) Hexa-μ_2-chloro-tetrakis(2-ethylpyrazine-*N*)-μ_4-oxo-tetracopper(II). Acta Crystallogr Sect E 58:m4–m6. https://doi.org/10.1107/S1600536801020438

Norman RE, Rose NJ (1989) Simple, direct synthesis and structure of Hexa-μ-chloro-tetrakis- (1-methylimidazole)-μ_4-oxo-tetracopper(II). Acta Crystallogr C 45:1707–1713. https://doi.org/10.1107/S0108270189002994

Ondrejovič G, Kotočová A (2006) Spectral and electrochemical study of coordination molecules $Cu_4OX_6L_4$: 3-pyridylmethanol and 4-pyridylmethanol Cu4OBrnCl(6-n)(pm)4 complexes. Chem Pap 60:198–206. https://doi.org/10.2478/s11696-006-0036-6

Ondrejovič G, Moncoľ J (2015) Structures of $Cu_4OCl_6L_4$ complexes studied by vector analysis. Book of Abstracts—XXV. International conference on coordination and bioinorganic chemistry, Smolenice: 101

Ondrejovič G, Moncoľ J (2017) Advanced structural analysis of coordination $Cu_4OX_6L_4$ molecules. Book of Abstracts—XXVI. International conference on coordination and bioinorganic chemistry, smolenice: 82

Ondrejovič G, Broškovičová A, Kotočová A (2000) Construction and structure of coordination polymers based on tetragonal Cu_4OBr 6 centres linked by pyrazine. Chem Pap 54:6–11

Parkin A, Barr G, Dong W, Gilmore CJ, Jayalitaka D, McKinnon JJ, Spackman MA, Wilson CC (2007) Comparing entire crystal structures: structural genetic fingerprinting. CrystEngComm 9:648–652. https://doi.org/10.1039/B704177B

Richardson C, Steel PJ (2003) Benzotriazole as a structural component in chelating and bridging heterocyclic ligands; ruthenium, palladium, copper and silver complexes. Dalton Trans 2003:992–1000. https://doi.org/10.1039/B206990C

Sheldrick GM (2015a) *SHELXT*—Integrated space-group and crystal-structure determination. Acta Crystallogr A 71:3–8. https://doi.org/10.1107/S2053273314026370

Sheldrick GM (2015b) Crystal structure refinement with *SHELXL*. Acta Crystallogr C 71:3–8. https://doi.org/10.1107/S2053229614024218

Siemens XE (1990) Siemens analytical X–ray Instruments Inc. Madison, Wisconsin

Skorda K, Stamatatos TC, Vafiadis AP, Lithoxoidou AT, Terzis A, Perlepes SP, Mrozinski J, Raptopoulou CP, Plakatouras JC, Bakalbassis EG (2005) Copper(II) chloride/1-methylbenzotriazole chemistry: influence of various synthetic parameters on the product identity, structural and magnetic characterization, and quantum-chemical studies. Inorg Chim Acta 358:565–582. https://doi.org/10.1016/j.ica.2004.09.042

Spackman MA, Jayalitaka D (2009) Hirshfeld surface analysis. CrystEngComm 11:19–32. https://doi.org/10.1039/B818330A

Spackman MA, McKinnon JJ (2002) Fingerprinting intermolecular interactions in molecular crystals. CrystEngComm 4:378–392. https://doi.org/10.1039/B203191B

Stibrany RT, Potenza JA (2007) CCDC 666757: experimental crystal structure determination. https://doi.org/10.5517/ccqct95

Tosik A, Bukowska-Strzyzewska M, Mrozinski J (2009) Synthesis, magnetism and X-ray structure of μ_4-oxo-hexa-μ_2-chlorotetrakis(benzimidazole)copper(II). J Coord Chem 24:113–125. https://doi.org/10.1080/00958979109409454

Turner MJ, McKinnon JJ, Wolff SK, Gromwood DJ, Spackman PR, Jayalitaka D, Spackman MA (2017) CrystalExplorer17.5. The University of Western Australia, Crawley

Vafazadeh R, Willis AC (2016) Synthesis, structure and electrochemistry of tetranuclear oxygen-centered copper(II) clusters with acetylacetone and benz-pyrazole hydrolyzed derivatives as ligands. Acta Chim Slov 63:186–192. https://doi.org/10.17344/acsi.2016.2263

Vafazadeh R, Hasanzade N, Heidari MM, Willis AC (2015) Synthesis, structure characterization, DNA binding, and cleavage properties of mononuclear and tetranuclear cluster of copper(II) complexes. Acta Chim Slov 62:122–129. https://doi.org/10.17344/acsi.2014.797

van Albada GA, Ghazzali M, Al-Farhan K, Reedijk J (2011) Synthesis and crystal structure of (μ_4-oxido)hexakis(μ-chlorido) tetrakis(2-(3-pyridyl)ethane-1-ol)tetracopper(II). A compound with a unique hydrogen bond system stabilizing the network. Inorg Chem Commun 14:1149–1152. https://doi.org/10.1016/j.inoche.2011.04.010

Voitekhovich SV, Gaponik PN, Lyakhov AS, Filipova JV, Sukhanova AG, Sukhanov GT, Ivashkevich OA (2009) N-Alkylation of

4-nitro-1,2,3-triazole revisited. Detection and characterization of the N3-ethylation product, 1-ethyl-5-nitro-1,2,3-triazole. Tetrahedron Lett 50:2577–2579. https://doi.org/10.1016/j.tetlet.2009.03.076

Yamada K, Oguma E, Nakagawa H, Kawazura H (1994) Structure of μ-Oxo-tetranuclear Copper(II) complex produced from chlorpromazine (cpz) and Cu(II)Cl_2. An alternative binding site of the cpz molecule to metal. Chem Pharm Bull 42:368–370. https://doi.org/10.1248/cpb.42.368

Zhang G, Yang C, Liu E, Golen J, Rheingold AL (2014) Mild, green copper/4-dimethylaminopyridine catalysed aerobic oxidation of alcohols mediated by nitroxyl radicals in water. RSC Adv 4:61907–61911. https://doi.org/10.1039/c4ra13929a